

Introduction: The application of interferometric techniques provides a substantial improvement of imaging speed as compared to conventional spectroscopic imaging [1,2]. This abstract outlines the sources of information that make interferometric MR imaging advantageous. Understanding these sources clarifies the algorithm, its assumptions, and its limitations.

Theory: For spectroscopic MR imaging, a desired image, $s(\vec{r}, f)$, can be characterized by collecting data $S(\vec{k}, t)$ which is related by the Fourier transform. In interferometric MRI, the data from two different k-space locations are cross-correlated temporally to produce the *mutual coherence function*.

$$\Gamma(\vec{k}_1, \vec{k}_2, \tau) = \int S(\vec{k}_1, t) S^*(\vec{k}_2, t - \tau) dt \quad (1)$$

By application of the van Cittert and Zernike theorem, the resulting correlation becomes equivalent to the Fourier transform of the original image squared (Chap. 14 of [3]).

$$\Gamma(\Delta\vec{k}, \tau) = \iint |s(\vec{r}, f)|^2 e^{-j\Delta\vec{k} \cdot \vec{r}} e^{-j\omega\tau} d\vec{r} df \quad (2)$$

This new correlation domain is mapped by $\Delta\vec{k} = \vec{k}_1 - \vec{k}_2$. For every N original locations of k-space, up to $N(N-1)$ locations of $\Delta\vec{k}$ are provided.

Methods and Discussion: The van Cittert and Zernike theorem relies on spatial incoherence. Any two voxels that oscillate at the same frequency will interfere and confound each other. To avoid this for any single spin species, a gradient is applied during the readout. An example of a 1-D spectroscopic sample is shown in Fig. 1, where the proposed method is able to reconstruct the data using a fraction of the phase encodes.

The dependence on spatial incoherence requires sparsity in the spectral domain. Different species of spin will interfere with other voxels depending on spectral separation and gradient strength. This interference can exhibit itself as 'ghosting' that is similar to some aliasing artifacts. Fig. 2 presents a simulation where two different species are mapped for a spectroscopic image with a gradient in the y-direction. The second spin species causes a ghost artifact Fig. 2 (c,d). The larger circle presents a large ghost in the interferometric reconstructions. A stronger gradient would spread out the ghosts until they would no longer fall within the field of view. Alternatively, lower acceleration would also mitigate the coherence artifact as it provides averaging across $\Delta\vec{k}$.

By directly imaging the square of the image, the proposed method exhibits phase ambiguity. The phase ambiguity presents a reduction of the degrees of freedom in the system by a factor of two.

Conclusions: Sources of information for interferometric MR imaging primarily originate from spectral sparsity and phase ambiguity. A trade-off exists between spectral separation of different spin species and non-destructive acceleration from the proposed method. While

interferometric MR imaging is constrained by spectral sparsity and phase ambiguity, it provides a new method for MR data acquisition. This technique may provide an alternative framework for imaging sparse systems

in both MRSI and conventional MR imaging. **References:** [1] Johnson and Meyer. 2011. *ISMRM*, 384. [2] Johnson, 2011. *BASP Frontiers*, [3] Thompson et al., 2001. *Interferometry and Synthesis in Radio Astronomy*. **Acknowledgements:** NIH R01HL079110, NIH T32HL007284

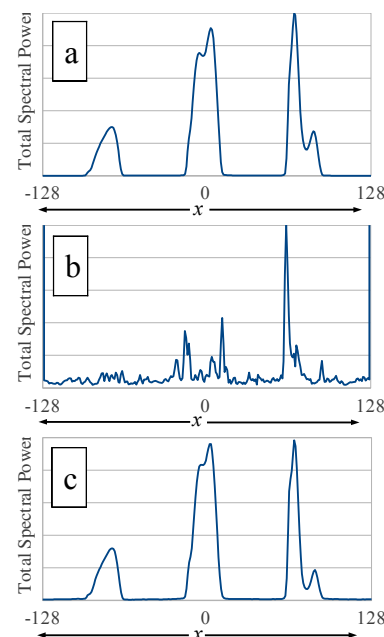


Fig. 1: Total spectral power for each voxel in a 1-D spectroscopic image. The three profiles represent test tubes as collected by scanner. (a) represents a conventional MRSI using 257 phase encodes. In both (b) and (c) the proposed technique is implemented using 39 phase encodes without a readout gradient (b) and with a gradient (c) to provide incoherence. Without the incoherence, the voxels confound in a destructive manner (b).

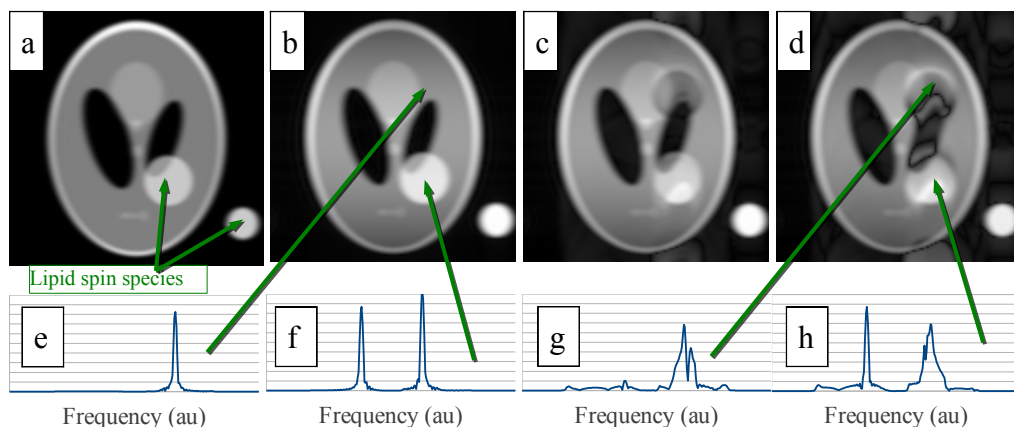


Fig. 2: Simulation for a 2-D MRSI using two spin species. Each image represents a sum through the spectra. Reconstruction from conventional MRSI using 63x127 phase encodes (a). The proposed technique is applied using 63x63 phase encodes (b), using 63x30 phase encodes (c) or 63x25 phase encodes (d) providing an effective R of 2, 4.2 or 5.1. Coherence artifact, evident as a 'ghost', is apparent in (c) and (d). As more data are used, the coherence artifact is reduced (b). A stronger gradient would push the ghost out past the field of view. Spectra from two voxels of (b) and (d) are presented in (e-h). The lipid spectra from (h) interferes with the water spectra of (g). A Hann window is applied to all 3 dimensions of each dataset.